Szczepan OPACH, Tomasz WOLNIK

Łukasiewicz Research Network – Upper Silesian Institute of Technology

doi:10.15199/48.2023.12.45

Parametrization of the thermal model of induction motor with outer rotor

Abstract. *This paper presents a method of parameterization of the thermal model of an electric motor on the example of an external rotor induction motor with high power density. The simulations presented in this paper were carried out on the motor model with a copper rotor cage with a rated power 25 kW and a mass of 16 kg. This construction, due to the demanding operating conditions they are subjected to, require precise thermal analysis at the design stage. In many works, this analysis is usually limited to thermal simulations without taking into account the rotating elements of the motor. This article presents a method of numerical determination of selected parameters of the CFD model, including the value of the heat transfer coefficient through the air gap, taking into account the rotational motion of the rotor, the convection coefficient, describing the intensity of convective heat exchange of the outer surface of the rotor body with the environment, and an alternative method of numerical determination of substitute values stator winding thermal conductivity coefficients. Based on the results obtained in numerical simulations, a three-dimensional CFD model of the motor was developed and solved.*

Streszczenie. *W publikacji przedstawiono sposób parametryzacji modelu cieplnego silnika elektrycznego na przykładzie silnika indukcyjnego z wirnikiem zewnętrznym o dużej gęstości mocy. Przedstawione w niniejszej pracy symulacje przeprowadzono na modelu sinika z miedzianą klatką wirnika o mocy znamionowej 25 kW i masie 16 kg. Tego rodzaju konstrukcje, ze względu na wymagające warunki eksploatacji, jakim są poddawane, wymagają precyzyjnej analizy termicznej na etapie projektowania. W wielu pracach analiza ta ogranicza się zwykle do symulacji termicznych bez uwzględnienia wirujących elementów maszyny. W niniejszym artykule zaprezentowano metodę numerycznego wyznaczania wybranych parametrów modelu CFD, w tym wartości współczynnika przenikania ciepła przez szczelinę powietrzną z uwzględnieniem ruchu obrotowego wirnika, współczynnika przejmowania ciepła, opisującego intensywność konwekcyjnej wymiany ciepła zewnętrznej powierzchni obudowy wirnika z otoczeniem oraz przedstawiono alternatywną metodę numerycznego wyznaczania wartości zastępczych współczynników przewodzenia ciepła uzwojenia stojana. Na podstawie wyników uzyskanych w symulacjach numerycznych opracowano i rozwiązano trójwymiarowy model CFD silnika.* (***Parametryzacja modelu termicznego silnika indukcyjnego z wirnikiem zewnętrznym***)

Słowa kluczowe: symulacje CFD, model cieplny, silnik indukcyjny, silniki o dużej gęstości mocy.
Keywords: CFD simulation, thermal model, induction motor, high power density motor.

Introduction

One of the directions in recent years is the development of high-efficiency electric drives independent of rare-earth permanent magnets [1-5]. This also applies to drives where the so-called Specific Power [kW/kg], informing about the power density of a given machine [1,4,6]. In addition, the increasing requirements for electric machines in recent years in terms of noise reduction, reliability, and ultimately also the cost of materials and production, forces the optimization of their design [7-8]. Of course, in terms of technology and operating parameters, motors with permanent magnets basically have no competition and are characterized by the best properties. However, taking into account the whole spectrum of important issues, including diversification of key components and independence from the global monopoly, there is a renewed interest in the development and improvement of other types of machines, including induction motors. An important issue in the design phase of motors is a properly developed thermal model of the motor and thermal simulations [6,9,10]. High power density motors operate under conditions of high current loads, often [12 - 15 A/mm^2] and high supply voltage frequencies [800 - 1000 Hz], so the components of the mechanical structure of these machines are particularly exposed to the negative thermal effects [11-12]. These include windings, bearings, permanent magnets, shaft seals and encoders [9]. The influence of heat on the electric machine should also be taken into account when selecting parts fits, assembly clearances or designing connections. The influence of the thermal state of the electric machine on its efficiency is also significant [9,13].

Currently, in many scientific works, attention is paid to thermal calculations of electric machines intended for the electromobility sector (automotive, aviation, shipping) [6,14,15]. In addition, the issue of thermal calculations is particularly important in the case of designing motors with high Specific Power. In these calculations, CFD thermal-flow simulations are used to determine the steady-state thermal state of an electric machine subjected to load at any operating point (e.g. rated or overloaded). CFD calculations also enable the intensification of heat removal from the electric machine by optimizing the efficiency of the cooling system.

Three-dimensional CDF models are developed on the basis of previously prepared and appropriately simplified three-dimensional CAD models and the characteristics of the construction materials used, including:

- thermal conductivity of the material λ (W/mK),
- specific heat of the material Cp (J/kgK),
- material density ρ (kg/m^3),
- dynamic viscosity of a liquid η (kg/ms),
- kinematic viscosity of a liquid v (m^2/s).

In addition, the CFD model is prepared taking into account the so-called boundary conditions of the task, such as:

- ambient temperature T_a (°C),
- coolant flow per unit of time F (kg/s),
- temperature T_{in} (°C) or fluid pressure P_{in} (bar) at the inlet of the cooling system,
- natural convection coefficients α_n (W/m^{2}K) and forced convection coefficients α_f (W/m^{2}K),
- heat transfer coefficients through the model's thermal barriers k (W/m^{2}K) or their reciprocal thermal resistances of thermal barriers Rt (m^{2}K/W).

The thermal load of the model, i.e. the value of power losses ΔP (W), expresses the amount of thermal energy generated in individual parts of the electrical machine per time unit. The most common value is the power loss in:

- stator winding ΔP_{Cus} (W),
- stator core ΔP_{Fes} (W),
- rotor winding ΔP_{Cur} (W),
- rotor core ΔP_{Fer} (W),
- mechanical losses in bearings ΔP_b.

Most materials (steel, aluminum, copper) on the basis of which CFD models of electrical machines are prepared show isotropy of heat conduction in all directions and can be defined by a constant thermal conductivity coefficient λ (W/mK). Non-homogenous (heterogeneous) parts and assemblies, which include windings, stator and rotor cores, have a composite (multi-layer) structure. In terms of thermal conductivity, they are orthotropic, i.e. thermal conductivity coefficients λ can be defined in three mutually perpendicular axes of the coordinate system (coinciding with the main axes of the machine). When preparing CFD models of composite (heterogeneous) structures, their geometries are simplified to homogeneous structures by assigning them newly created materials, defined by the thermal conductivity coefficient in three mutually perpendicular directions λ_x, λ_y, λ_z. When defining the material for a homogeneous model of windings and cores, a constant thermal conductivity coefficient is assumed in the plane normal to the main axis of the machine $\lambda_x = \lambda_y = \lambda_{xy}$ and a significantly different thermal conductivity coefficient in the direction of the main axis of the machine λ_z, and in the case of the winding model $\lambda_{xy} << \lambda_z$, and in the case of the core package model $\lambda_{xy} >> \lambda_z$.

In recent years, many experimental studies have been carried out to determine the equivalent heat conduction coefficients for windings λ_{SWxy}, λ_{SWz}, and cores λ_{COxy}, λ_{COz}, and to determine the value of thermal resistance Rt of thermal partitions between individual parts of an electric machine [10,13,16]. Similar results can be achieved using numerical simulations [17,18]. In the case of winding, two-dimensional models are usually made in order to represent the real composite structure of the material in the cross-section of the slot. Thus, it is possible to model the arrangement of the winding wires in the space of the slot assuming the appropriate filling factor, and also to take into account the actual diameter of the winding wire, the thickness of the enamel layer and filling slot with impregnating varnish. The simulation then consists in numerically determining the value of the thermal flux q (W), caused by the temperature difference $\Delta T = T_2 - T_1$ (°C), on two opposite sides of the slot and analytical determination of the substitute heat conduction coefficient λ_{xy} (Equation (1)).

$$\lambda_{xy} = \frac{q \cdot l}{S \cdot \Delta T} \tag{1}$$

where: l – distance of planes to which temperature boundary conditions T_1 and T_2 have been assigned,
S – surface area of the plane to which temperature boundary conditions T_1 and T_2 have been assigned.

The literature provides the values of thermal conductivity coefficients for the slot filling materials (enamel, impregnation varnish), used to build numerical models [19]. However, there are no examples illustrating the method of modeling the heat exchange between the stator and the rotor of an electric machine in spatial CDF models. The meshing of the air gap model based on the finite element method is troublesome because the dimensions of the gap in comparison with the overall dimensions of the machine are small. This causes an undesirable increase in the mesh quality parameter, the so-called Aspect Ratio, i.e. the ratio of the size of the largest to the smallest finite elements of the model. To avoid this problem, publication [20] proposed a method of building three-dimensional CFD models without modeling and meshing of the air gap. The author presents a method of numerical determination of the thermal resistance of the air gap Rt_{ag} (m^{2}K/W), taking into account the rotational motion of the rotor. The thermal resistance value obtained in this way is used in the definition of the contact between the cylindrical surface of the stator and the rotor. In publication [21] the authors use an analytical method of determining the equivalent value of the thermal resistance of the air gap. Experience shows that the results obtained by numerical and analytical methods are consistent with each other and can be used alternatively.
When developing three-dimensional CFD models of electric machines with an internal rotor, the constant (taking form the literature) values of the natural convection coefficient α_n (W/m2K) and forced convection coefficient α_f (W/m2K), are most often assumed. In the case of electric machines with an external rotor, especially those operating at high rotational speed, such a simplification may result in inaccuracy of the obtained simulation results. The coefficient of convection α_f forced by the rotational motion of the rotor of electric machines with an external rotor should be determined each time not only in relation to the geometry of the machine, but also depending on its rotational speed.

This article presents a method of numerical determination of the value of the heat transfer coefficient k_{ag} (W/m^{2}K) through the air gap of the motor, taking into account the rotational motion of the rotor. A method of numerical determination of the convection coefficient α_f (W/m^{2}K) describing the intensity of convective heat exchange of the outer surface of the rotor body with the environment was presented. The method of numerical determination of substitute values of the thermal conductivity coefficients λ_{xy} and λ_z of the stator winding was also presented. Based on the results obtained in numerical simulations, a three-dimensional CFD model of an induction motor with an external rotor and a copper cage with a rated power of P_n = 25 kW, rotating at a speed of 8000 rpm, was developed and solved. The aim of the simulations carried out was to find out the steady-state temperature of all motor components. In addition, the intensity of heat removal from the motor by the coolant was analyzed. The average temperature of the cooling medium at the outlet of the cooling system T_{out} was determined, and the temperature increase of the cooling liquid $\Delta T = T_{out} - T_{in}$ was also examined.

The model of induction motor

The input data for the thermal model in the form of power losses generated in motor components are obtained from electromagnetic calculations. The subject of analysis in this paper is a model of induction motor with an external rotor with a copper cage (Fig.1). Table 1 shows the basic data and parameters of the motor model. Table 2 presents the calculated values of power losses, which in the next steps were implemented in the CFD model. Both the electromagnetic calculations and the subsequent thermal simulations were carried out for the rated operating point of the motor.

Table 1. Parameters of the induction motor model

Parameter			
Rated power	P_n	kW	25
Rated torque	T_n	Nm	30.3
Rated rot. speed	n_n	rpm	7890
Rated voltage	U_{LL}	V	400
Rated current	I_n	A	50.9
Efficiency	η	%	91.8
Power factor	$cos\varphi$	-	0.78
Number of poles	$2p$	-	8
Number of phases	m	-	3

Figure 2 shows the operating characteristics of the Torque vs. rotational speed at 400 V, 533.33 Hz. The maximum torque of the motor is 60 Nm.

Table 2. Power losses in the motor model

Parameter			
Stator winding losses	ΔP_{Cus}	W	1000
Stator core losses	ΔP_{Fes}	W	650
Losses in bars of rotor	ΔP_{Br}	W	300
Losses in shorting rings in rotor	ΔP_{Sr}	W	150

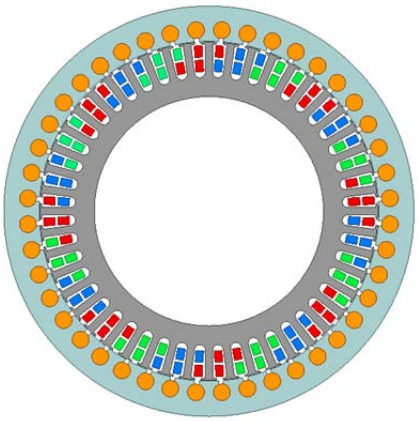

Fig.1. Electromagnetic circuit model of an external rotor induction motor.

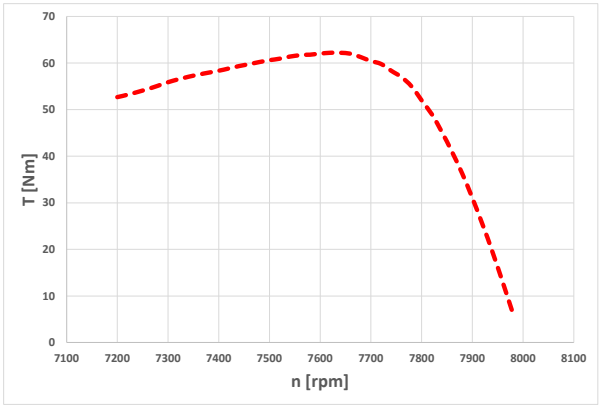

Fig.2. Torque vs. rotational speed characteristics.

Construction and meshing of the CAD model

The three-dimensional model of the motor, previously prepared in the CAD software, was subjected to appropriate simplification and then meshing by a finite element method in the ANSYS 2021 R2 Fluent software. Figure 3 shows the CAD model of the motor.

Fig.3. CAD model of an induction motor with an external rotor

The thermal-flow model includes all main parts and assemblies of the motor, including:

- an external rotor assembly containing a rotor core with a copper cage, press-fitted into the aluminum, rotating rotor housing,
- an internal stator assembly containing a wound stator core, press fit mounted on the aluminum body in which a liquid cooling system is located,
- a shaft mounted on two bearings inside the body, coupled with the rotating body of the rotor.

The model of the stator core, the rotor core, the stator winding as well as the short-circuit rings and rotor cage bars were meshing based on hexahedral finite elements using the sweep method with a density of 1 element for every 1 mm of model length. The stator winding model consists of the straight bars with a cross-section corresponding to the cross-section of the slot, extended outside the stator core to the length resulting from the pitch of the winding (and not from the overhang of the winding end-conection). This is a new approach to modeling the stator winding, allowing to avoid the error resulting from the incorrect definition of the directions of thermal conductivity in the winding face in traditional modeling. The remaining parts of the model: body elements, shaft and bearings were meshed based on 5 mm hexahedral finite elements. The meshing effect of the 3D model of the induction motor with an external rotor is shown in the Figure 4.

The coolant model in the cooling system was meshed using the inflation method with 3 boundary layers and the Increase Factor of 1.2. Boundary layer modeling allows for accurate simulation of the liquids behavior in layers adjacent to the walls. The inner layer of the liquid was meshed based on 2 mm hexahedral elements. The meshing effect of the 3D model of the cooling liquid is shown in Figure 5.

Fig.4. Motor model with a finite element mesh in ANSYS software

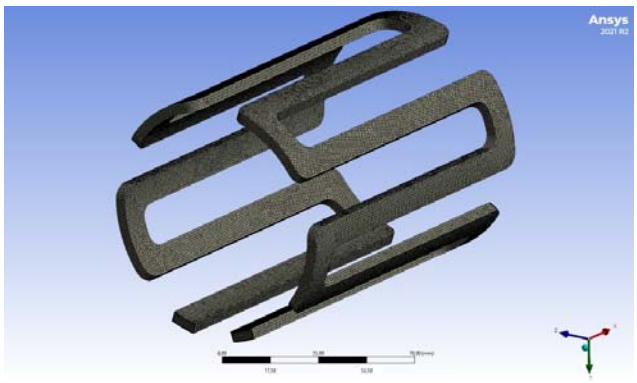

Fig.5. Coollant with a finite element mesh in ANSYS software

The air gap model was not meshed. At the stage of preparing the 3D model of the motor, the outer diameter of

the stator core was equalized with the inner diameter of the rotor core (Fig. 6). At a later stage - parameterization of the thermal-flow model, the contact created at the contact between the stator and the rotor was defined with the value of the equivalent thermal resistance of the air gap, taking into account the rotational motion of the rotor.

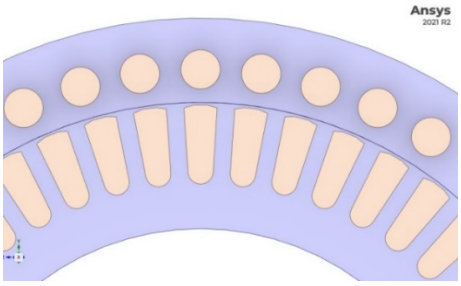

Fig.6. A simplified model of the stator and rotor of the induction motor with the air gap omitted

Heat transfer coefficient through the air gap

In order to determine the equivalent value of the thermal resistance of the air gap, a numerical method described in the literature was used [20]. Computational three-dimensional (3D) numerical model of the air gap were prepared based on the Finite Element Method in ANSYS 2021 R2 Fluent software. The model was prepare based on hexahedral finite elements with 8 nodes, arranged along the air gap using the sweep method with a density of 2 elements for every 1 mm of the gap length. In the cross-section of the gap, the elements were arranged evenly in 4 layers. The model makes it possible to assign the rotational speed n (RPM) to one of the two cylindrical surfaces of the gap: external for the case of an external rotor or internal for the case of an internal rotor. The meshing effect of the 3D model of the air gap is shown in the Figure 7.

Table 3. Air material parameters taken from the ANSYS Fluent material database

Density	ρ_{air}	1.225	kg/m^3
Specific heat	Cp_{air}	1006.43	J/(kgK)
Thermal conductivity	λ_{air}	0.024	W/(mK)
Dynamic viscosity	η	$17.89 \cdot 10^{-6}$	kg/(ms)
Kinematic viscosity	v	$14.61 \cdot 10^{-6}$	m^2/s

The boundary conditions of the task are: rotor rotational speed n (rpm) and two arbitrarily selected values of temperatures T_1 and T_2 (°C), respectively assigned to two cylindrical surfaces of the model. The effect of the temperature difference $\Delta T = T_2 - T_1$ (°C) is the heat flux q (W) occurring between the surface of the stator and the rotor, the direction of which is opposite to the temperature gradient. In the simulation, the case of an external rotor rotating at a given speed of n = 8000 rpm was tested for several selected ΔT values. For each case, the value of the heat flux q (W) was calculated, and then the values of the heat transfer coefficients k_{ag} (W/m^{2}K) and the inverse values of the equivalent thermal resistances Rt_{ag} (m^{2}K/W) were determined (Formula (2)).

$$k_{ag} = \frac{1}{Rt_{ag}} = \frac{q}{S \cdot \Delta T} \tag{2}$$

The value of the heat transfer coefficients through the air gap k_{ag} does not depend on the temperature difference ΔT (°C), but strictly depends on the set rotor rotational speed n (rpm). The calculated value of the equivalent thermal resistance of the air gap Rt_{ag} = 0.00773 m^{2}K/W was used to parameterize the thermal-flow model of the induction motor.

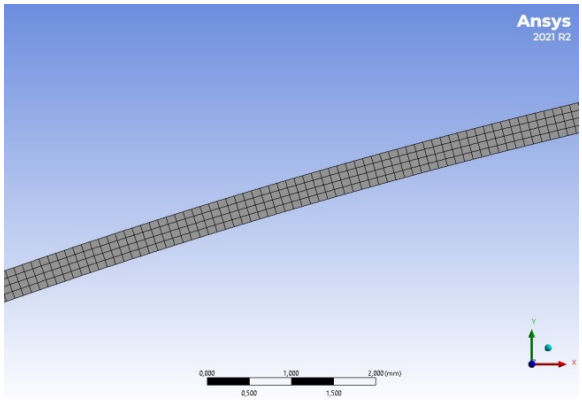

Fig.7. 3D model of an air gap with a finite element mesh in ANSYS

Forced convection coefficient for the outer surface of the rotor body

The numerical two-dimensional (2D) model was built and solved in the ANSYS 2021 R2 Fluent software. In the two-dimensional model, the thickness parameter was defined - specifying the actual length of the rotor. The modeled airspace around the rotor is a circle with a diameter of 3 m. It was assumed that at a distance of 1.5 m from the rotor axis, the influence of the heat generated by the motor on the ambient temperature T_a (°C) is negligible, and thus temperature boundary condition T_a = 22°C.

The second boundary condition of the task - the temperature T_1 was defined on the outer surface of the rotor. For four exemplary values of $\Delta T = T_a - T_1$ (°C), numerical simulations were carried out, during which the values of the heat flux q (W) were tested, the direction of which is opposite to the temperature gradient. In addition, two cases of the rotational speed n = 4000 rpm and the rated speed n = 8000 rpm were tested.

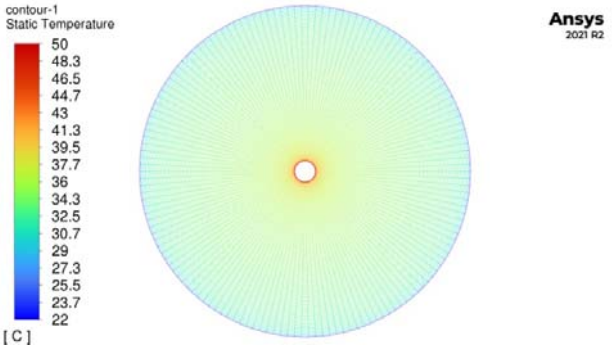

Fig.8. Temperature distribution around the rotor for n = 8000 rpm.

The purpose of the simulations was to determine the value of the forced convection coefficient α_f (m^{2}K/W) - the so-called coefficient of convection forced by the rotation of the rotor. As a result of the simulations, the values of the unit heat flux $\dot{q}$ (W/m^2) were determined for each of the discussed cases. The corresponding values of forced convection coefficients α_f were calculated using the formula:

Based on the results presented in Table 4 and Table 5, it was shown that the value of forced convection coefficient α_f does not depend on the temperature difference ΔT (°C), but strictly depends on the rotational speed n. The calculated value of the forced convection coefficient α_f = 58.43 W/m^{2}K was used to parameterize the CFD model of the motor.

$$\alpha_f = \frac{\dot{q}}{\Delta T} \tag{3}$$

Table 4. Calculated values of forced convection coefficient α_f for rotational speed n = 8000 rpm

T_1 (°C)	T_a (°C)	ΔT (°C)	$\dot{q}$ (W/m^2)	α_f (W/m^{2}K)
125	22	103	6018.8	58.43
100	22	78	4557.9	58.43
75	22	53	3097.0	58.43
50	22	28	1636.2	58.43

Table 5. Calculated values of forced convection coefficient α_f for rotational speed n = 4000 rpm

T_1 (°C)	T_a (°C)	ΔT (°C)	$\dot{q}$ (W/m^2)	α_f (W/m^{2}K)
125	22	103	3374.4	32.76
100	22	78	2555.4	32.76
75	22	53	1736.3	32.76
50	22	28	917.3	32.76

Equivalent thermal conductivity coefficient of the stator winding in the slot cross-section

Computational two-dimensional (2D) numerical models were prepared based on the Finite Element Method in ANSYS 2021 R2 (Steady State Thermal) software. A copper round winding wire with diameters d'= 1.279 mm and d = 1.180 mm was selected for the simulation. Two variants of winding wire arrangement in the stator slot were investigated. In the first "square" variant the centres of adjacent wires were placed at the vertices of the square so that the gap between the wires was 0.02 mm. In the second "triangle" variant the centres of the adjacent wires were placed at the vertices of an equilateral triangle keeping the same gap as before. Additionally simulations were performed with a slot filled with impregnating varnish and air. The models took into account the composite geometric and material structure of the stator slot filling: copper, enamel, impregnation varnish (or air). It was assumed that in terms of thermal conductivity all the materials used are isotropic and their specific thermal conductivity coefficients are:

- copper : λ_{Cu} = 385 W/mK,
- enamel : λ_{en} = 0.23 W/mK,
- impregnating varnish : λ_{iv} = 0.3 W/mK,
- air : λ_{air} = 0.024 W/mK.

The winding samples were modeled in such a way as to make them repeatable in both axes of the plane of the stator slot cross-section. Thus there is no need to model the entire cross section of the slot and the method is universal. The values of the equivalent thermal conductivity coefficient λ_{xy} (W/mK) obtained from the calculations are a material feature of the winding constructed on the basis of a specific winding wire and placed in a slot with a specific slot filling factor. Its value is not influenced by the shape and dimensions of the stator slot.

The boundary conditions of the calculation model are two constant temperature values assigned to the opposite edges of the sample T_1 and T_2 (°C). The calculations were completed when the temperature field in the entire calculation area of the model was established. The purpose of the calculations was to determine the value of the heat flux (W) between two opposite edges of the sample for which boundary conditions were defined, i.e. the value of thermal power flowing between the edge of the sample by higher and lower temperature. With the heat flux q (W) and the geometrical dimensions of the sample: length l (m) and the boundary condition surface area S (m^2) as well as the value of the temperature difference ΔT (°C) the values of the equivalent thermal conductivity coefficient in the sample λ_{xy} (W/mK) were determined using Formula 1.

It should be noted that the geometry of the calculation model was designed in the scale of 100:1 in relation to the geometric dimensions of the real sample what does not affect the value of the coefficient λ_{xy} (W/mK) because the heat power q (W) flowing through the sample is proportional to its geometrical dimensions and λ_{xy} (W/mK) is a constant proportionality factor characteristic for the structure of the material used. The calculations were performed for the case of arranging the winding wire in the stator slot in a "square" and "triangle" method. For both cases calculations were carried out taking into account the filling of the stator slot with impregnating varnish and air and for several different temperatures T_1 and T_2 (°C).

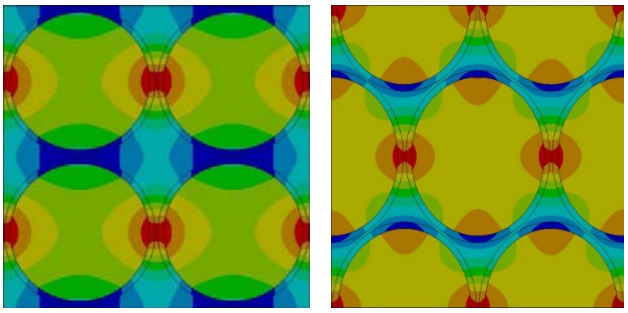

Fig.9. Temperature distribution in the tested sample in the "square" and "triangle" configuration with filling of the slot with the impregnating varnish

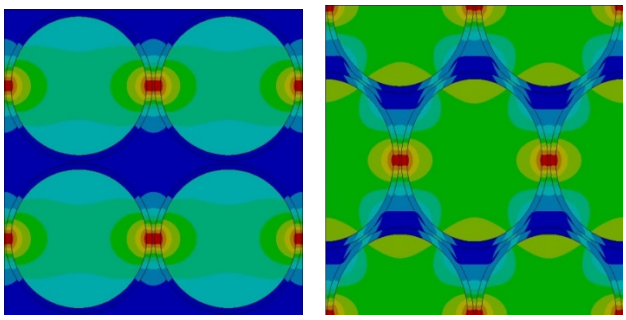

Fig.10. Temperature distribution in the tested sample in the "square" and "triangle" configuration with filling of the slot with the air

The results of calculations collected in the Tables 6-9 confirm that the value of the equivalent thermal conductivity coefficient λ_{xy} (W/mK) does not depend on the values of T_1 and T_2 (°C) temperatures as it is a material feature independent of the boundary conditions of the task. However it can be seen that the value of the coefficient λ_{xy} (W/mK) varies depending on the configuration of the winding wire arrangement in the slot and depending on the material used to fill the slot (impregnating varnish, air).

Table 6. Input data and calculation result for the "square" configuration with filling of the slot with the impregnating varnish

q (W)	S (m^2)	l (m)	T_1 (°C)	T_2 (°C)	ΔT (°C)	λ_{xy} (W/mK)
139.12	0,2598	0.2598	20	120	100	1.39
243.46	0,2598	0.2598	0	175	175	1.39
115.47	0,2598	0.2598	38	121	83	1.39
27.82	0,2598	0.2598	20	40	20	1.39

Table 7. Input data and calculation result for the "triangle" configuration with filling of the slot with the impregnating varnish

q (W)	S (m^2)	l (m)	T_1 (°C)	T_2 (°C)	ΔT (°C)	λ_{xy} (W/mK)
158.33	0.2250	0.2598	20	120	100	1.83
277.08	0.2250	0.2598	0	175	175	1.83
131.41	0.2250	0.2598	38	121	83	1.83
31.7	0.2250	0.2598	20	40	20	1.83

Table 8. Input data and calculation result for the "square" configuration with filling of the slot with the air

q (W)	S (m^2)	l (m)	T_1 (°C)	T_2 (°C)	ΔT (°C)	λ_{xy} (W/mK)
32.03	0.2598	0.2598	20	120	100	0.32
56.05	0.2598	0.2598	0	175	175	0.32
26.58	0.2598	0.2598	38	121	83	0.32
6.40	0.2598	0.2598	20	40	20	0.32

Table 9. Input data and calculation result for the "triangle" configuration with filling of the slot with the air

q (W)	S (m^2)	l (m)	T_1 (°C)	T_2 (°C)	ΔT (°C)	λ_{xy} (W/mK)
42.30	0.2250	0.2598	20	120	100	0.49
74.02	0.2250	0.2598	0	175	175	0.49
35.11	0.2250	0.2598	38	121	83	0.49
8.46	0.2250	0.2598	20	40	20	0.49

The calculated value of the equivalent thermal conductivity coefficient λ_{xy} = 1.39 W/mK was used to parameterize the CFD model of the induction motor.

Parameterization and solution of the 3D CFD model

The values of equivalent heat conduction λ, heat transfer k and convection coefficient α, obtained in the numerical simulations described in the previous chapters, were used to parameterize the three-dimensional CFD model of the analyzed induction motor. The values of the remaining coefficients were taken from the records of the analyzed literature and experiments. First, the materials were defined in the database and assigned to individual parts of the model, with particular emphasis on the value of thermal conductivity coefficients λ.

Table 10. Values of thermal conductivity coefficients for the construction materials of the model

Motor element	Material	Thermal conductivity
Stator body, rotor body	Aluminium PA4	λ_{Al} = 185 W/mK
Shaft, bearings	Steel	λ_{St} = 58 W/mK
Shorting rings, rotor cage bars	Copper	λ_{Cu} = 385 W/mK
Stator winding	Composite	λ_{SWxy} = 1,39 W/mK λ_{SWz} = 385 W/mK
Stator core, rotor core	Composite	λ_{COxy} = 25 W/mK λ_{COz} = 3 W/mK

Next, the values of equivalent thermal resistances Rt (m^2K/W) were analytically determined for the contacts representing the sliding connections of the parts of the motor model. This case concerns the sliding connection of the rolling bearings with the body hubs $Rt_{b\text{-}b}$ (m^2K/W) and bars of the cage with holes in the rotor core $Rt_{b\text{-}c}$ (m^2K/W). It has been assumed that for small air gaps (hundredths of a millimetre), heat transmission through the gap is by conduction only and the following formula can be used (RC_{max} - the maximum radial clearance of the connection, λ_{air} = 0,024 W/mK). For example, in the case of connecting bars with holes in the rotor core, the following can be written:

$$Rt_{b-c} = \frac{RC_{max}}{\lambda_{air}} = \frac{0{,}025\cdot10^{-3}m}{0{,}024\frac{W}{mK}} = 0.00104\,\frac{m^2K}{W} \quad (4)$$

In a similar way, the value of the thermal resistance of the slot insulation of the stator was calculated. $Rt_{w\text{-}c}$ (m^2K/W), constituting a thermal barrier for heat transfer from the winding towards the stator core. The parameterization of the model assumed the use of slot insulation with a thickness g_{si} = 0.25 mm and thermal conductivity λ_{si} = 0.14 W/mK, which gives the value of thermal resistance:

$$Rt_{w-c} = \frac{g_{si}}{\lambda_{si}} = \frac{0{,}25\cdot10^{-3}m}{0{,}14\frac{W}{mK}} = 0.00178\,\frac{m^2K}{W} \quad (5)$$

The values of all thermal resistances calculated and taken from the literature for contacts occurring in the parameterized CFD model of the motor are presented in Table 11.

Table 11. Values of equivalent thermal resistances of connections used in model parameterization.

Motor element	Symbol	Thermal resistance
bearing - body (sliding connection)	$Rt_{b\text{-}b}$	0.00059 (m2K/W)
bearing - shaft (press fit)	$Rt_{b\text{-}s}$	0.00015 (m2K/W)
winding – stator core (slot insulation)	$Rt_{w\text{-}c}$	0.00178 (m2K/W)
stator/rotor core - body (press fit)	$Rt_{c\text{-}b}$	0.00015 (m2K/W)
cage bars - rotor core (sliding connection)	$Rt_{b\text{-}c}$	0.00104 (m2K/W)
air gap	Rt_{ag}	0.00773 (m2K/W)
cage bars - rotor shorting rings (solder connection)	$Rt_{b\text{-}sr}$	0 (m2K/W)

When parameterizing the CFD model, the following values of the convection coefficients, the so-called coefficients of natural convection from the outer surface of the housing and forced convection from the rotating rotor body (n = 8000 rpm) were assumed:
natural convection coefficient α_n = 15 W/m^2K
forced convection coefficient α_f = 58,5 W/m^2K

The CFD simulation of the analyzed induction motor was carried out assuming the following values of the boundary conditions of the task:

- coolant flow per unit of time: F = 8 l /min (~0.133 kg/s),
- temperature at the inlet of the cooling system T_{in} = 15 °C,
- ambient temperature T_a = 22°C.

The load on the model is represented by the values of power losses ΔP (W) in motor elements, whose values resulting from the previously performed electromagnetic calculations are presented in Chapter 2. The results of the simulations carried out are presented in the Figures 11-Figure 16.

The intensity of heat removal generated in the motor by the coolant was subjected to additional analysis. The distribution of fixed temperatures of the cooling medium (water) obtained in the CFD simulation is shown on the solid model and on the exit plane of the cooling system in the Figure 17.

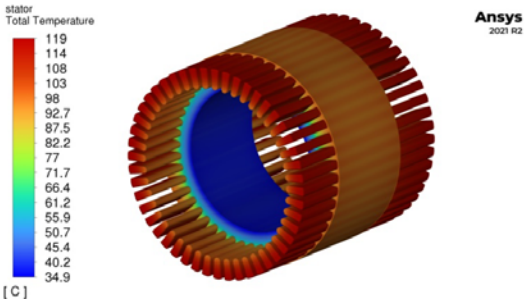

Fig.11. Caluclated thermal steady state in winding and stator core

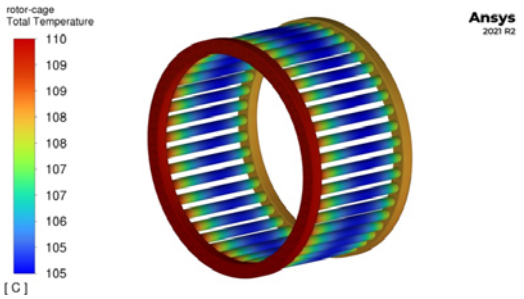

Fig.12. Caluclated thermal steady state in cooper cage

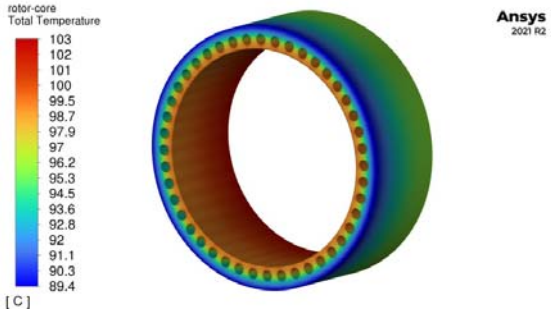

Fig.13. Caluclated thermal steady state in rotor core

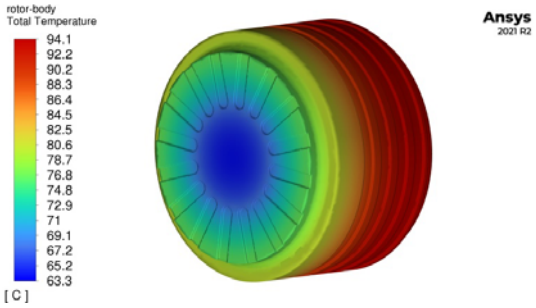

Fig.14. Caluclated thermal steady state in the rotor housing

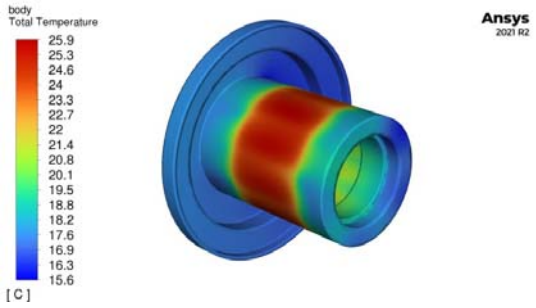

Fig.15. Caluclated thermal steady state in the stator housing

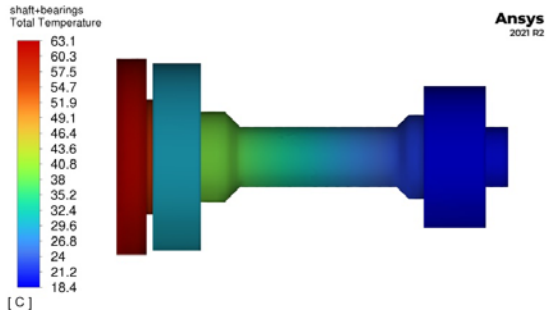

Fig.16. Calculated thermal steady state in the shaft and bearings

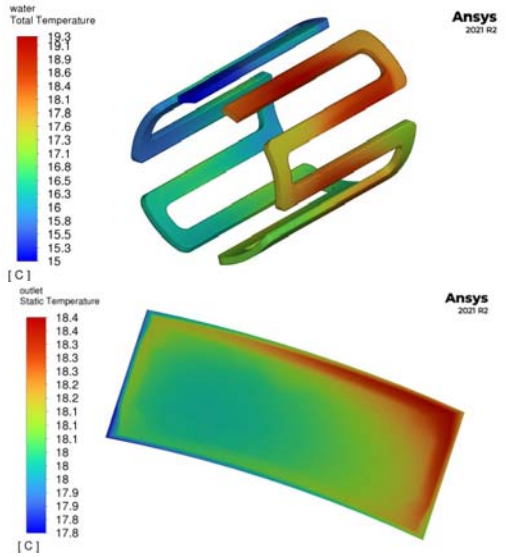

Fig.17. Calculated thermal steady state of coolant (water)

The analysis of the temperature distribution of the cooling medium, and in particular the measurement of the average temperature at the outlet of the cooling system, gives the possibility of initial verification of the accuracy of the performed thermal and flow calculations. Knowing the value of power losses ΔP of a liquid-cooled electric machine, it is possible, omitting the influence of convective heat exchange with the environment, to determine the average temperature T_{out} (°C) at the outlet of the cooling system.

More accurate calculations can be made by analyzing the thermal power balance in the model, which is also the result of the CFD simulation. The point here is to determine the real value of the thermal power transferred by convection to the motor's surroundings from the surface of the machine (Formula 6). From the thermal power balance of the model, it can be read that as a result of forced convection from the surface of the rotor housing to the environment of the motor, 378.8 W of power is transferred. For comparison, as a result of natural convection from the housing surface to the environment of the motor, only 3.0 W of power is transferred.

(6) $$T_{out}{}^{*} = \frac{\Delta P - \Delta P_C}{Cp\frac{F}{60}} + T_{in} = \frac{1720{,}2}{4182\frac{8}{60}} + 15 = 18.1\ ^{\circ}C$$

The results obtained by analytical calculations and formula 6 prove the correctness of the developed model, the adopted parameterization and the method of calculating the heat transfer path P (W) from the sources of its generation to the place of its exchange with the environment. It should also be noted that the temperature difference at the inlet and outlet of the cooling system is only 3.1 °C. The result suggests that the proposed shape of the cooling system channel is close to optimal and allows for efficient dissipation of thermal power generated in the motor to the environment.

Conclusion

This article presents a method of parameterization of a thermal model of an external rotor induction motor with high power density. A method of numerical determination of selected parameters of the CFD model was presented, including the value of the heat transfer coefficient through the air gap, taking into account the rotational motion of the rotor, the heat transfer coefficient describing the intensity of convection heat exchange of the outer surface of the rotor

housing with the environment and an alternative method of numerical determination of substitute values of thermal conductivity coefficients stator windings. The partial results obtained were compared with the results obtained from analytical calculations. These results are consistent.

This paper was supported and financed by The National Center for Research and Development (NCBR - Poland), project "Silniki elektryczne o dużej gęstości mocy", LIDER/31/0169/L-12/20/NCBR/2021.

***Authors**:*
M.Sc.ME. Szczepan Opach
E-mail: szczepan.opach@git.lukasiewicz.gov.pl
Ph.D.EE. Tomasz Wolnik
E-mail: tomasz.wolnik@git.lukasiewicz.gov.pl
Łukasiewicz Research Network – Upper Silesian Institute of Technology, Karola Miarki 12-14, 44-100 Gliwice

REFERENCES

[1] A. Chiba, K. Kiyota, N. Hoshi, M. Takemoto, and S. Ogasawara, 'Development of a Rare-Earth-Free SR Motor With High Torque Density for Hybrid Vehicles', IEEE Trans. Energy Convers., vol. 30, no. 1, pp. 175–182, Mar. 2015, doi: 10.1109/TEC.2014.2343962.

[2] M. Morimoto, 'Iron loss of non-rare earth traction motor for electric vehicle', in 2010 IEEE Vehicle Power and Propulsion Conference, Lille, France: IEEE, Sep. 2010, pp. 1–4. doi: 10.1109/VPPC.2010.5729030.

[3] N. G. Ozcelik, U. E. Dogru, M. Imeryuz, and L. T. Ergene, 'Synchronous Reluctance Motor vs. Induction Motor at Low-Power Industrial Applications: Design and Comparison', Energies, vol. 12, no. 11, p. 2190, Jun. 2019, doi: 10.3390/en12112190.

[4] J. D. Widmer, R. Martin, and M. Kimiabeigi, 'Electric vehicle traction motors without rare earth magnets', Sustainable Materials and Technologies, vol. 3, pp. 7–13, Apr. 2015, doi: 10.1016/j.susmat.2015.02.001.

[5] T. Wolnik, P. Dukalski, B. Będkowski, T. Jarek 'Selected aspects of designing motor for direct vehicle wheel drive', Przeglad Elektrotechniczny, vol. 1, no. 4, pp. 152–155, Apr. 2020, doi: 10.15199/48.2020.04.31.

[6] Y. Xia, Y. Han, Y. Xu, and M. Ai, 'Analyzing Temperature Rise and Fluid Flow of High-Power-Density and High-Voltage Induction Motor in the Starting Process', IEEE Access, vol. 7, pp. 35588–35595, 2019, doi: 10.1109/ACCESS.2019.2899346.

[7] P. Dukalski and R. Krok, 'Selected Aspects of Decreasing Weight of Motor Dedicated to Wheel Hub Assembly by Increasing Number of Magnetic Poles', Energies, vol. 14, no. 4, p. 917, Feb. 2021, doi: 10.3390/en14040917.

[8] T. Wolnik, V. Styskala, and T. Mlcak, 'Study on the Selection of the Number of Magnetic Poles and the Slot-Pole Combinations in Fractional Slot PMSM Motor with a High Power Density', Energies, vol. 15, no. 1, p. 215, Dec. 2021, doi: 10.3390/en15010215.

[9] J. Madej and B. Będkowski, 'Air flow analysis for electrical motor's cooling system with autodesk simulation CDF 2013 program', Acta Mechanica et Automatica, vol. 7, no. 2, pp. 89–92, Jun. 2013, doi: 10.2478/ama-2013-0016.

[10] B. Będkowski and J. Madej, 'The innovative design concept of thermal model for the calculation of the electromagnetic circuit of rotating electrical machines', Eksploatacja i Niezawodność, vol. 17, no. 4, pp. 481–486, Sep. 2015, doi: 10.17531/ein.2015.4.1.

[11] T. Wolnik, 'LEMoK – silnik o dużej gęstości mocy', Maszyny Elektryczne - Zeszyty Problemowe, no. 1(127), 2022, pp. 107-110.

[12] T. Wolnik, T. Jarek, J. Golec, R. Topolewski, and D. Jastrzębski, 'High Power Density Motor for Light Electric Aircraft – Design Study and Lab Tests', in 2023 IEEE Workshop on Electrical Machines Design, Control and Diagnosis (WEMDCD), Newcastle upon Tyne, United Kingdom: IEEE, Apr. 2023, pp. 1–6. doi: 10.1109/WEMDCD55819.2023.10110934.

[13] B. Bedkowski, P. Dukalski, T. Jarek, and T. Wolnik, 'Numerical model for thermal calculation analysis of the wheel hub motor for electric car verified by laboratory tests', IOP Conf. Ser.: Mater. Sci. Eng., vol. 710, no. 1, p. 012018, Dec. 2019, doi: 10.1088/1757-899X/710/1/012018.

[14] P. Dukalski and B. Będkowski, 'Obliczenia cieplne silnika elektrycznego do zabudowy w piaście koła samochodu' Napędy i Sterowanie, vol. 24, no.7/8, pp. 70-76.

[15] Ł. Cyganik and B. Będkowski, 'Układ mechaniczny przełączania zazębienia pomiędzy silnikiem elektrycznym, przekładnią planetarną oraz piastę koła w napędzie elektrycznym zabudowanym w kole pojazdu' Maszyny Elektryczne - Zeszyty Problemowe, no. 1(127), 2022, pp. 117-122.

[16] B. Będkowski, J. Madej, 'Wyznaczenie zastępczej rezystancji cieplnej izolacji żłobkowej – badania I symulacje' Maszyny Elektryczne - Zeszyty Problemowe, 2(106), 2015, pp. 117-122.

[17] P. Mynarek, 'Zastosowanie metody homogenizacji do wyznaczania współczynnika przewodnictwa cieplnego w silnikach elektrycznych', Przegląd Elektrotechniczny, vol. 1, no. 1, pp. 183–186, Jan. 2017, doi: 10.15199/48.2017.01.44.

[18] P. Mynarek and M. Kowol, 'Metoda homogenizacji uzwojeń wsypywanych w maszynach elektrycznych' Maszyny Elektryczne - Zeszyty Problemowe, 1(105), 2015, pp. 149-154.

[19] G. Kondziołka, 'Kryteria doboru syciw oraz lakierów elektroizolacyjnych' Maszyny Elektryczne - Zeszyty Problemowe, 2(102), 2014, pp. 7-10.

[20] S. Opach, 'Obliczenia wartości zastępczej rezystancji cieplnej szczeliny powietrznej w wirnikowych maszynach elektrycznych, Maszyny Elektryczne - Zeszyty Problemowe, no. 1(127), 2022, pp. 101-105.

[21] D. A. Howey, P. R. N. Childs, and A. S. Holmes, 'Air-Gap Convection in Rotating Electrical Machines', IEEE Trans. Ind. Electron., vol. 59, no. 3, pp. 1367–1375, Mar. 2012, doi: 10.1109/TIE.2010.2100337.